Full Paper

Propellants, Explosives, Pyrotechnics

DOI: 10.1002/prep.201700235

Effect of Boron-Containing Hydrogen-Storage-Alloy ($Mg(BH_x)_y$) on Thermal Decomposition Behavior and Thermal Hazards of Nitrate Explosives

Dandan Ji,[a] Xiaoan Wei,*[a] Ping Du,[a] Guanyong Zhang,[a] and Zeshan Wang[a]

Abstract: Thermal decomposition properties and hazards of nitrate explosives containing $Mg(BH_x)_y$ were investigated by thermogravimetry-differential scanning calorimetry (TG-DSC), accelerating rate calorimeter (ARC) and characteristic drop height impact sensitivity tests. Results show that the addition of $Mg(BH_x)_y$ to nitrate explosives led to increase in the volatilization temperature of nitroglycerine in the nitrate explosive. It was not the thermolysis product of $Mg(BH_x)_y$, but $Mg(BH_x)_y$ itself acted on the nitrate explosive in the TG-DSC tests. Kinetic parameters and thermal hazard assessment parameters were calculated based on ARC data. Results show that a mixture of the nitrate explosive with $Mg(BH_x)_y$ had higher apparent activation energy and lower thermal hazard. Experiments of characteristic drop height showed that $Mg(BH_x)_y$ reduced the impact sensitivity of nitrate explosives.

Keywords: $Mg(BH_x)_y$ · nitrate explosive · TG-DSC · ARC · impact sensitivity

1 Introduction

In order to improve the destructive power, high-energy additives are used in explosives [1, 2]. Metal hydrides as hydrogen storage materials, although their research and development are not for the purpose of energetic materials, are expected to be fuel components. The reason is that metal hydrides have high reactivity, and release large amounts of heat in the combustion processes [3, 4, 5]. Magnesium-based hydrides are characterized by, for example, high hydrogen storage density, high energy, low pollution, good thermal stability, etc. Nitrate explosives occupy an important place in the propellant fields [6, 7]. Adding metal hydride materials is beneficial for the development of the military and space industry. Many scholars have carried out researches on the hydrogen absorption and desorption of magnesium-based hydrogen storage materials and their applications in energetic materials.

Higuchi [8] investigated the temperature corresponding to the maximum dehydrogenation rate, which was remarkably shifted to lower temperature with the increase in the thickness of the nano-composite three-layered Pd/Mg/Pd film prepared by an RF-associated magnetron sputtering method. Wahab [9] et al. revealed a synergetic effect of nanoconfinement with catalysis by Ni nanoparticles on $Mg(BH_4)_2$, which allows the hydrogen release to initiate at a temperature of only 75 °C and the release rate to significantly increase. Nielsen [10] pointed out that kinetic improvement of hydrogen absorption and desorption occurs when the MgH_2 nanoparticles are less than 50 nm in size, and thermodynamic improvement occurs for smaller MgH_2 nanoparticles with a size less than 5 nm. Chlopek and Hanada et al. [11, 12] synthesized magnesium tetrahydroborate in several ways and investigated its thermal decomposition under He flow and H_2 pressure. Yao et al. studied the effect of magnesium hydride powder on the thermal decomposition behaviors based on RDX and TNT [13, 14]. Jin et al. investigated the influence of MgH_2 on the thermal decomposition properties of nitrocellulose [15]. However, the effects of metal hydrides on the thermal decomposition properties, thermal hazards and impact sensitivity of nitrate explosives remain to be further studied, which are important for transportation and application.

In this research, $Mg(BH_x)_y$ as a high energetic material was added to nitrate explosives to prepare energy explosives. TG-DSC and ARC experiments were performed to investigate the thermodynamic performance of thermal decomposition. Effects of dynamic performance and thermal hazards were analyzed based on curves and data. The effect of impact sensitivity was studied by characteristic drop height experiments.

[a] *D. Ji, X. Wei, P. Du, G. Zhang, Z. Wang*
School of Chemical Engineering
Nanjing University of Science & Technology
Nanjing, Jiangsu 210094, P.R. China
**e-mail: weixiaoan@126.com*

2 Experimental

2.1 Materials

$Mg(BH_x)_y$ was prepared by ion exchange in the liquid phase, and its stability was improved by coating treatment. The corning process is described in the following. First, 400 g nitrate explosive were mixed by a kneader using 70 mL acetone as solvent. After 30 min, 10 mL acetone was added into the kneader in which $Mg(BH_x)_y$ was dispersed. 3.5 h later, the dough was obtained and added into the forming mold. Through an extrusion molding process, a strand was received and left for 48 h. Finally, the strand was cut into grains.

The nitrate ester explosive contents 50 percent of nitrocellulose (N% = 12.5), 49 percent of nitroglycerine, and 1 percent of explosion regulator. Formulae of explosives are listed in Table 1.

Table 1. Formula of nitrate explosives.

ID	Component	Mass ratio
1#	Nitrate ester	100
2#	Nitrate ester:$Mg(BH_x)_y$	92:8 ~ 95:5

2.2 Experimental Equipment and Conditions

A TG-DSC apparatus from NETZSCH (Model: STA449C) was used in this study. Samples (about 1 mg) were tested under a dynamic argon atmosphere at a flow rate of 30 mL min^{-1} and a heating rate of 10 °C min^{-1}. Sample 1# decomposed completely at 500 °C, so the temperature range of sample 1# was 0 ~ 500 °C, while the temperature range of sample 2# was 0 ~ 900 °C.

An ARC apparatus from THT (Model: esARC) was used to test a large quantity of the samples. Experiments were performed at the atmospheric pressure, a heating rate of 5 °C min^{-1}, a latency time of 10 min, and a detection sensitivity of 0.02 °C min^{-1}. Test conditions are shown in Table 2.

Table 2. Test condition.

ID	Sample mass [g]	Bomb mass [g]	Initial temperature [°C]
1#	0.101	14.427	40
2#	0.092	8.961	40

The characteristic drop height experiment and the calculation were carried out according to GJB772A (601.2) [16]. The hammer was 2 kg. Since the nitrate explosive with the hydrogen material had high energy and caused serious damage to the instrument, each sample was reduced to about 50 mg.

3 Results and Discussion

3.1 TG-DSC

Nitrate explosives and $Mg(BH_x)_y$ have a negative oxygen balance. An oxygen-free state appeared in the thermal decomposition process under a dynamic argon atmosphere in TG-DSC. TG-DSC curves of the two samples are shown in Figure 1.The results of TG-DSC are listed in Table 3 and Table 4.

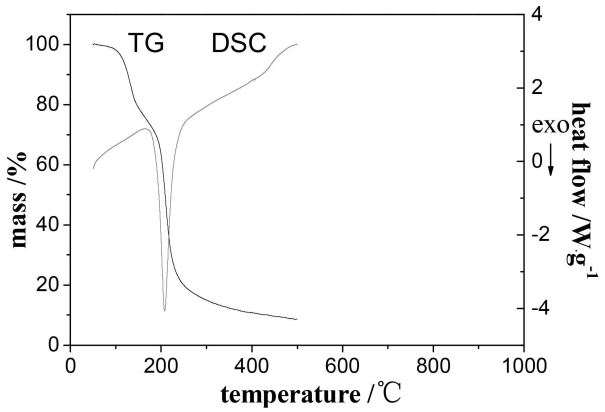

(a) TG-DSC curves of sample 1#

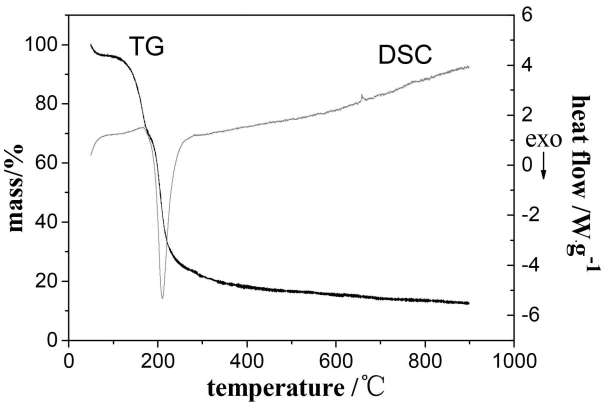

(b) TG-DSC curves of sample 2#

Figure 1. TG-DSC results.

Table 3. TG results.

ID	T_1 [°C]	T_2 [°C]	η [%]
1#	110.7	196.9	91.3
2#	142.9	195.8	83.0

Table 4. DSC results.

ID	T_0 [°C]	T_p [°C]	Q [J·g^{-1}]
1#	192.26	207.7	1319
2#	190.24	210.6	1259

It can be seen that both the nitrate explosive and the mixture of nitrate explosive with $Mg(BH_x)_y$ have two steps in the weight loss. For the nitrate explosive, the initial decomposition temperature of the first step is 110.7 °C and the initial decomposition temperature of the second step is 196.9 °C. The initial decomposition of the mixture of nitrate explosive with $Mg(BH_x)_y$ is delayed until 142.9 °C and the initial decomposition temperature of the second step is 195.8 °C. In the first process, the nitroglycerin in the nitrate explosive volatilizes with heat. Because of the large specific surface area of $Mg(BH_x)_y$, a part of nitroglycerin generated in the first decomposition process is adsorbed, leading to increase in the onset temperature of the weight loss for the first time.

Figure 1 shows that nitrate ester has an exothermic decomposition peak at 207.7 °C. The exothermic decomposition peak appears slightly later due to the addition of $Mg(BH_x)_y$. A small endothermic peak appears at 657.5 °C in Figure 1 (b). Under a dynamic argon atmosphere, the nitrate explosive burns completely at about 277 °C. According to the literatures, the decomposition of $Mg(BH_x)_y$ is initiated at about 290 °C. The decomposition products cannot burn because the system is oxygen-free. No weight loss occurs at a relevant position of the TG curve at 657.5 °C and the heat release is 60 J/g^{-1} lower, indicating that the cause of the endothermic process is not the decomposition of $Mg(BH_x)_y$, but the melting of Mg.

Table 4 shows that, as compared with the nitrate ester, the peak temperature of the mixture of nitrate ester with $Mg(BH_x)_y$ increases by 3 °C while the heat reduces by 4.5 %. The oxygen balance value is −0.11 g·g^{-1} for the nitrate ester and −2.8 g·g^{-1} for $Mg(BH_x)_y$. $Mg(BH_x)_y$ decomposed and could not obtain enough oxygen to burn in the TG-DSC experiment, thus the apparent heat of the mixture of nitrate explosive with $Mg(BH_x)_y$ decreased. The results of TG-DSC tests indicated that not the thermolysis products of $Mg(BH_x)_y$ but $Mg(BH_x)_y$ itself worked to delay the occurrence of initial decomposition and improved the thermal stability of the nitrate explosive.

3.2 Test by Accelerating Rate Calorimeter

ARC experiments provide mass data, such as the temperature, time, pressure, temperature increase rate and pressure increase rate. The activation energy, reaction order, pre-exponential factor and the material heat sensitivity can be obtained by analysis of the original data [17].

3.2.1 Thermodynamic Analysis by ARC

The heat generated from the reaction heats both the sample itself and the reaction bomb. Therefore, in order to obtain accurate data, the original data need to be corrected with the thermal inertia factor (φ) [18].

Decomposition reaction curves of the two samples are shown in Figure 2. The corrected thermal decomposition data are listed in Table 5.

In the ARC experiment, the heat released by the thermal decomposition of the mixture of nitrate explosive with $Mg(BH_x)_y$ was far higher than the heat supplied by system. The temperature rise rate was out of the sensitivity range of the instrument, so the latter part of thermal decomposition of the mixture of nitrate ester with $Mg(BH_x)_y$ was not analyzed. It can be seen from the curves in Figure 2 (a) and Figure 2 (b) that, releases of the heat and the gas occur simultaneously, and the variation trends are basically consistent in the adiabatic decomposition process. Figure 2 (a) shows that the temperature of the mixture of nitrate ester with $Mg(BH_x)_y$ is significantly higher than the nitrate ester. The pressure suddenly increases and then decreases at about 160 °C ~ 170 °C, leading to the change in the adiabatic decomposition curves of the mixture of nitrate explosive with $Mg(BH_x)_y$ as shown in Figure 2(b). Correspondingly, the curves of the pressure increase rate vs. temperature and the temperature increase rate vs. temperature slightly rise in

Table 5. Adiabatic decomposition data.

Parameter	1# Original data	1# Corrected data (φ = 31.00)	2# Original data	2# Corrected data (φ = 26.52)
T_0 [°C]	140.73	–	146.21	–
T_f [°C]	182.00	1419.87	197.44	1504.80
ΔT_{ad} [°C]	41.27	1279.14	51.23	1358.60
m_0 [°C·min^{-1}]	0.045	1.39	0.17	4.56
m_m [°C·min^{-1}]	1.03	32.05	50.15	1329.90
θ_m [min]	144.41	4.66	18.76	0.71
P_m [MPa]	0.92	–	1.41	–
Q [J·g^{-1}]		2558.28		2717.19

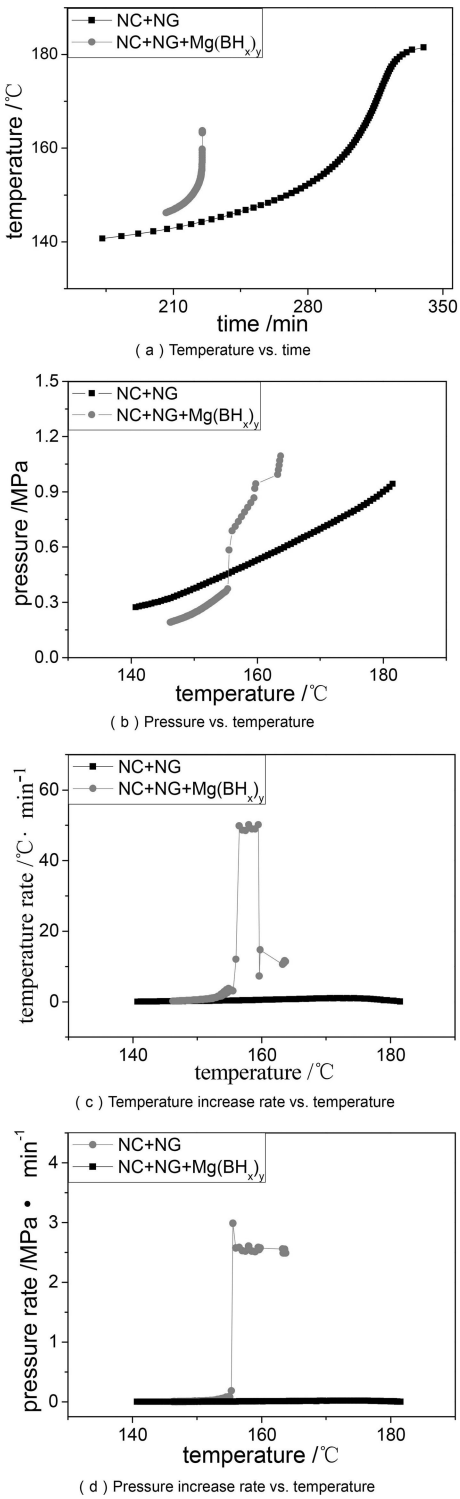

Figure 2. Adiabatic decomposition curves by ARC.

the temperature range as shown in Figure 2 (c) and Figure 2 (d). The phenomenon may be caused by the large quantities of combustible gases produced by decomposition of the mixture of nitrate ester with $Mg(BH_x)_y$ at about 160 °C ~ 170 °C.

As shown in Table 5, the initial decomposition temperature T_0 of the nitrate ester is 140.73 °C and the initial increase rate of temperature m_0 is 1.39 °C min^{-1}. After the addition of $Mg(BH_x)_y$, the initial decomposition temperature T_0 increased by 5.48 °C and the initial increase rate of temperature m_0 raised up to 4.56 °C min^{-1}. This means that, as compared with the nitrate ester, the stability of the mixture of the nitrate explosive with $Mg(BH_x)_y$ is improved significantly, and $Mg(BH_x)_y$ changes the heat release rate of the nitrate ester. Adiabatic temperature rise T_{ad} is proportional to the energy released by the samples. The addition of $Mg(BH_x)_y$ increased the adiabatic temperature T_{ad} rise from 1279.14 °C to 1358.6 °C, while the heat Q increased by 158.91 J·g^{-1}, indicating that energy of the mixture was increased. The maximal increase rate of temperature m_m of the nitrate ester is 32.05 °C min^{-1} and the maximal increase rate of temperature m_m of the mixture of the nitrate explosive with $Mg(BH_x)_y$ is 40.49 times higher, which means that $Mg(BH_x)_y$ raises the energy release rate of the mixture.

In ARC experiments, $Mg(BH_x)_y$ improved the decomposition temperature of the nitrate ester. The nitrate ester released substantial heat which led to decomposition of $Mg(BH_x)_y$ after the decomposition. The oxygen content in the bomb was much higher than that in DSC experiments, $Mg(BH_x)_y$ decomposed and the products participated in combustion reactions, so that the reaction rate was increased and a large amount of heat was released.

3.2.2 Dynamic Analysis by ARC

A temperature rate equation in the ARC experiment can be expressed as follow:

$$m_T = \frac{dT}{dt} = kc_0^{n-1}\left(\frac{T_f - T}{\Delta T_{ad}}\right)^n \Delta T_{ad} \quad (1)$$

k^* is the pseudo zero-order rate constant which is used to calculate the kinetic parameters.

$$k^* = kc_0^{n-1} = \frac{dT}{dt}\left(\frac{T_f - T_0}{\Delta T_{ad}}\right)^{-n} \Delta T_{ad}^{-1} \quad (2)$$

$$\ln k^* = \ln(Ac_0^{n-1}) - \frac{Ea}{RT} \quad (3)$$

After a proper reaction order is chosen, the plot of $\ln k^*$ vs. $1/T$ should be a straight line. From the slope and the intercept of the line, the Arrhenius kinetic parameters (E_a, A) can be calculated. The plots of $\ln k$ vs. $1000/T$ and linear fitting curves are shown in Figure 3, and calculated results of kinetic parameters of the thermal decomposition are listed in Table 6.

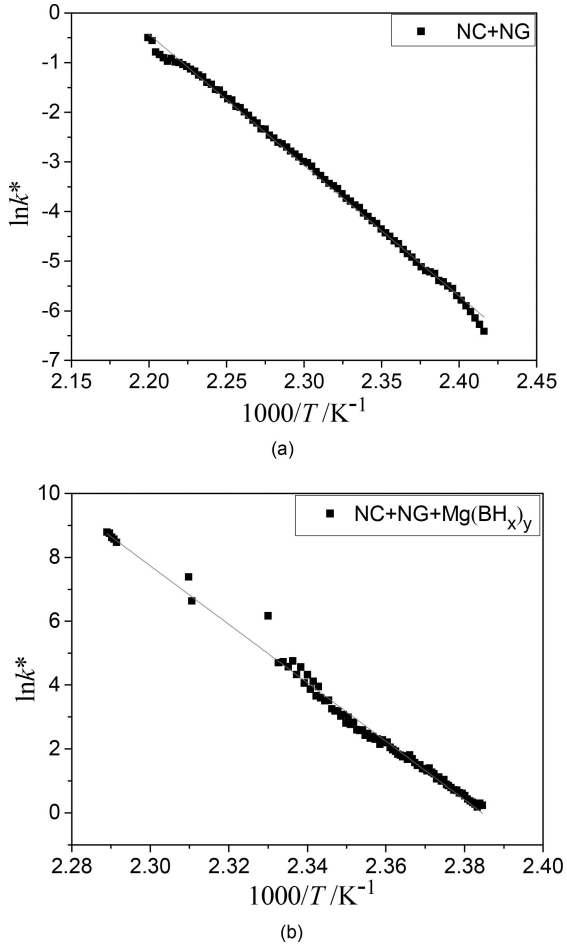

Figure 3. ln k^* vs. 1000/T.

Table 6. Kinetic parameters of thermal decomposition.

ID	E_a [kJ·mol^{-1}]	A [s^{-1}]	n	R^2
1#	219.24	1.026E25	1.2	0.997
2#	761.02	6.15E94	3	0.990

Note: The parameters listed in the table are calculated based on the test data which are for reference only.

It can be seen from Figure 3 and Table 6 that, when $Mg(BH_x)_y$ is added, E_a and A are significantly increased, which means that the addition of $Mg(BH_x)_y$ makes the thermal decomposition of the nitrate explosive more difficult to be initiated. The reaction order of the mixture of nitrate explosive is higher than that of the nitrate explosive, indicating that $Mg(BH_x)_y$ accelerates the thermal decomposition of nitrate ester, and makes the reaction more violent. The fact that $Mg(BH_x)_y$ makes the reaction more difficult to be initiated does not contradict the acceleration once the reaction is initiated.

3.2.3 Analysis of Thermal Hazards by ARC

The self-accelerating decomposition temperature (T_{SADT}), no return temperature (T_{NR}) and the corresponding temperatures at 8 h and 24 h under adiabatic conditions (T_{D8}, T_{D24}) are main parameters of thermal hazard assessment.

$$\tau = \frac{M\overline{c_{vs}}}{US} \tag{4}$$

$$\ln(TMR_{ad}) = \frac{E_a}{R}\left(\frac{1}{T}\right) - \ln A \tag{5}$$

$$T_{SADT} = T_{NR} - \frac{RT_{NR}^2}{E_a} \tag{6}$$

When the apparent activation energy E_a and the pre-exponential factor A are known, the time constant can be calculated by Formula (4), and then T_{NR} can be obtained according to Formula (5) [19]. Using the same method, we can establish T_{D8} and T_{D24}. T_{SADT} can be calculated according to Formula (6) [20]. Results are listed in Table 7.

Table 7. Explosion temperature corresponding to different induction periods.

ID	T_{NR} [K]	T_{D8} [K]	T_{D24} [K]	T_{SADT} [K]
1#	392.97	388.60	382.41	387.12
2#	401.89	400.54	398.62	400.13

Table 7 indicates that the addition of $Mg(BH_x)_y$ can reduce thermal hazards of nitrate explosives since all results of the thermal hazard assessment of sample 2# increased. The calculated results are consistent with the kinetic parameters of ARC tests.

3.3 Test of Characteristic Drop Height of Impact Sensitivity

In the tests, the drop height was adjusted, and the height at which 50 % of the samples exploded was recorded. The height characterizes impact sensitivity of energetic materials. Results of 20 parallel tests are shown in Table 8.

Table 8. Results of tests of characteristic drop height

ID	H_{50} [cm]
1#	13.14
2#	16.98

In the tests of characteristic drop height, the impact sensitivity of explosives is closely related to the degree of diffi-

culty in the formation of hot spots. In the impact process, some crystals and particles gained energy through friction, collision and compression, and thus formed hot spots [21, 22]. As shown in Table 7, when $Mg(BH_x)_y$ is added into the nitrate explosives, the impact sensitivity decreases because $Mg(BH_x)_y$ has no explosive group and is insensitive after coating. The corning process allows $Mg(BH_x)_y$ to disperse uniformly in the nitrate explosives. The friction and shear stress of $Mg(BH_x)_y$ particles in the mixture are low or zero since the mass fraction of $Mg(BH_x)_y$ is low. Moreover, breaking of $Mg(BH_x)_y$ particles consumes a part of the energy. Impact force passes along the metal surfaces quickly and reduces the probability of formation of local hot spots. It can be known from the results of ARC that, high apparent activation energy of the mixture of nitrate explosive with $Mg(BH_x)_y$ may reduce impact sensitivity of nitrate explosives.

4 Conclusions

Thermal decomposition steps of nitrate explosives mixed with $Mg(BH_x)_y$ were investigated under a dynamic argon atmosphere. The addition of $Mg(BH_x)_y$ increased volatilization temperature of nitroglycerine in the nitrate explosive. After the decomposition of the nitrate explosive, there is no enough oxygen for the decomposition products of $Mg(BH_x)_y$. Therefore, $Mg(BH_x)_y$ has a less effect on the decomposition of the nitrate explosive in TG-DSC tests.

Results of the ARC tests show that, the addition of $Mg(BH_x)_y$ has improved the onset temperature of adiabatic decomposition, the temperature increase rate and the thermal decomposition rate of nitrate explosives. The addition of $Mg(BH_x)_y$ increases the apparent activation energy and the pre-exponential factor of the nitrate explosive. The increase in the reaction order indicates that the reaction rate of the thermal decomposition of the nitrate explosive increases. Thermal hazard parameters, T_{NR}, T_{SADT}, T_{D8} and T_{D24}, of nitrate explosives with $Mg(BH_x)_y$ are higher than those of the nitrate explosives. The impact sensitivity is decreased due to $Mg(BH_x)_y$ in the characteristic drop height tests as well in the ARC tests.

$Mg(BH_x)_y$ can improve the stability of nitrate explosives and make the thermal decomposition reaction difficult to initiate. However, once the decomposition reaction is initiated, the reaction rate will increase to which attentions should be paid in applications.

Symbols and Abbreviations

TG-DSC	Thermogravimetry and Differential scanning calorimertry
ARC	Accelerating rate calorimetry
MgH_2	Magnesium hydride
$Mg(BH_x)_y$	Boron-containing hydrogen storage alloy
T_1	Initial decomposition temperature of the first step in TG test [°C]
T_2	Initial decomposition temperature of the second step in TG test [°C]
η	Weight loss [%]
T_0	Initial decomposition temperature [°C]
T_p	Peak temperature [°C]
T_f	Final temperature [°C]
ΔT_{ad}	Adiabatic temperature rise [°C]
m_0	Initial increase rate of temperature [$°C \cdot min^{-1}$]
m_m	Maximal increase rate of temperature [$°C \cdot min^{-1}$]
P_m	Maximal pressure [MPa]
Q	Heat release [$J \cdot g^{-1}$]
φ	Thermal inertia
c_0	Initial concentration of reactant [%]
τ	Time constant [h]
n	Reaction order
R^2	Fitting degree
M	Mass of the capacity [kg]
U	Overall heat transfer coefficient [$J \cdot m^{-2} \cdot K^{-1}$]
S	Surface area [m^2]
$\overline{c_{vs}}$	Specific heat [$J \cdot kg^{-1} \cdot K^{-1}$]
TMR_{ad}	Time to maximum rate under adiabatic condition [h]
T_{NR}	Temperature of no return [K]
T_{SADT}	Self-accelerating decomposition temperature [K]
T_{D8}	Temperature corresponding to $TMR_{ad} = 8$ h [K]
T_{D24}	Temperature corresponding to $TMR_{ad} = 24$ h [K]

References

[1] N. Li, L. Q. Xiao, W. L. Zhou, F. M. Xu, Energy Characteristics Analysis of GAP-ETPE Propellant Formulations. *Chin. J. Explos. and Propellants* **2010**, *33*, 74–81.

[2] Y. F. Cheng, Q. Wang, Y. Gong, T. Y. Fu, H. P. Yuan, H. Qian, Z. W. Sheng, Preparation and Detonation Properties of MgH_2 Type of Composite Sensitized Emulsion Explosives. *CIESC J.* **2017**, *68*, 1734–1739.

[3] L. T. DeLuca, L. Rossettini, C. Kappenstein, V. Weiser, 45th AIAA/ASME/ASE/ASEE Joint Propulsion Conference and Exhibit, Denver, CO, USA, August 2–5, **2009**, Ballistic Characterization of AlH_3-based Propellants for Solid and Hybrid Rocket Propulsion. *AIAA Pap.* **2009**, 4874.

[4] J. R. Hradel, *Enhanced organic explosives*, US Patent 3,012,868, DOW Chemical Corporation. Midland, MI, USA, **1961**.

[5] V. Rosenband, A. Gany, A Microscopic and Analytic Study of Aluminum Particles Agglomeration. *Combust. Sci. Technol.* **2001**, *166*, 91–108.

[6] J. F. Yuan, H. J. Wei, H. Wang, B. Qu, X. L. Fu, Effect of Nitrate Ester on the Driving Ability of RDX-based Aluminized Explosive. *Chin. J. Explos. and Propellant* **2015**, *38*, 62–65.

[7] Y. F. Liu, H. X. Guan, W. S. Yao, M. X. Li, H. M. Tan, Effect of Components on Combustion Properties of Nitrate Ester Plasticized Polyether. *J. Propul. Technol.* **2005**, *26*, 364–366.

[8] K. Higuchi, K. Yamamoto, H. Kajioka, K. Toiyama, M. Honda, S. Orimo, H. Fujii, Remarkable Hydrogen Storage Properties in

Three-Layered Pd/Mg/Pd Thin Films. *J. Alloys Compd.* **2002**, *330*, 526–530.

[9] M. A. Wahab, Y. Jia, D. J. Yang, H. J. Zhao, X. D. Yao, Enhanced Hydrogen Desorption From $Mg(BH_4)_2$ by Combining Nanocofinement and Ni Catalyst. *J. Mater. Chem. A* **2013**, *1*, 3471–3478.

[10] T. K. Nielsen, F. Besenbacher, T. R. Jensen, Nanoconfined Hydrides for Energy Storage. *Nanoscale* **2011**, *3*, 2086–2098.

[11] K. Chlopek, C. Formmen, A. Léon, O. Zabara, M. Fichtner, Synthesis and Properties of Magnesium Tetrahydroborate, $Mg(BH_4)_2$. *J. Mater. Chem.* **2007**, *17*, 3496–3503.

[12] N. Hanada, K. Chlopek, C. Formmen, C. Frommen, W. Lohstroh, M. Fichtner, Thermal Decomposition of $Mg(BH_4)_2$ under He flow and H_2 pressure. *J. Mater. Chem.* **2008**, *18*, 2611–2614.

[13] M. Yao, L. P. Chen, J. H. Peng, Effects of $MgH_2/Mg(BH_4)_2$ Powers on the Thermal Decomposition Behaviors of 2,4,6-Trinitrotoluene(TNT). *Propellants Explos. Pyrotech.* **2015**, *40*, 197–202.

[14] M. Yao, L. P Chen, P. Du, J. H. Peng, Effect of $Mg(BH_4)_2$ and MgH_2 on Thermal Decomposition Performance of RDX. *China Saf. Sci. J.* **2013**, *23*, 115–120.

[15] L. M. Jin, P. Du, M. Yao, The influence of Magnesium Hydride on the Thermal Decomposition Properties of Nitrocellulose. *J. Energ. Mater.* **2014**, *32*, S13–S21.

[16] Explosive test method, GJB 772A-1997.

[17] X. M. Qian, L. Liu, J. Zhang, Accelerating rate calorimeter and its application in the thermal hazard evaluation of chemical production. *J. Saf. Sci. Technol.* **2005**, *1*, 13–18.

[18] D. I. Townsend, J. C. Tou, Thermal hazard evaluation by an accelerating rate calorimeter. *Thermochim. Acta* **1980**, *37*, 1–30.

[19] J. H. Sun, H. Ding, *Thermal Hazard Evaluation of Chemicals.* Science Press, Beijing, **2005**, p. 150–153.

[20] United nations. Recommendations on the transport of dangerous goods, manual of tests and criteria 3red revised edn. 1999.

[21] Y. C. Liu, J. H. Wang, C. W. An, Y. W.Yu, Effect of Particle Size of RDX on Mechanical Sensitivity. *Chin. J. Explos. and Propellants* **2004**, *27*, 7–9.

[22] S. M. Zhang, S. Q. Hu, H. X. Zhao, Preparation of Nano α-Al_2O_3 Powder and its Influence on the Impact Sensitivity of RDX. *Chin. J. Explos. and Propellants* **2008**, *31*, 25–27.

Received: September 28, 2017
Revised: December 6, 2017
Published online: February 20, 2018

